



1 Real-Time Estimation of Airflow Vector based on Lidar 2 Observations for Preview Control

3 Ryota Kikuchi¹, Takashi Misaka², Shigeru Obayashi³, Hamaki Inokuchi⁴

4
5 ¹DoerResearch Inc., Chiba 260-0013, Japan

6 ²National Institute of Advanced Industrial Science and Technology, Ibaraki 305-8564, Japan

7 ³Tohoku University, Miyagi 980-8577, Japan

8 ⁴Japan Aerospace Exploration Agency, Tokyo 181-0015, Japan

9 *Correspondence to:* Ryota Kikuchi (Email: kikuchi-ryota@doerresearch.com)

10 **Abstract.** The control technique in a gust alleviation system by using the airborne Doppler Lidar technology is
11 expected to enhance aviation safety to minimize the risks of turbulence-related accidents. Accurate measurement
12 and estimation of the vertical wind velocity are very important in the successful implementation of a gust alleviation
13 system by using the airborne Doppler Lidar technology. An estimation algorithm of airflow vector based on the
14 airborne Lidars is proposed and investigated for preview control to prevent turbulence-induced aircraft accidents in
15 flight. The use of the simple vector conversion method, which is an existing technique, assumes that the wind field
16 between the Lidars is homogeneous. The assumption of a homogeneous field would be wrong when turbulence
17 occurs due to large wind velocity fluctuation. The proposed algorithm stores the line-of-sight (LOS) wind data with
18 each passing moment and uses recent and past LOS wind data in order to estimate the airflow vector. The recent and
19 past LOS wind data are used to extrapolate the wind field between the airborne twin Lidars. Two numerical
20 experiments—ideal vortex model and numerical weather prediction—were conducted to evaluate the estimation
21 performance of the proposed method. The proposed method has much better performance than simple vector
22 conversion in the two numerical experiments, and it can estimate accurate two-dimensional wind field distributions
23 unlike simple vector conversion. The estimation performance and the computational cost of the proposed method
24 can satisfy the performance demand for preview control.

25 1 Introduction

26 Atmospheric turbulence poses a potential risk to aircraft operation, and an increase in the rate of accidents
27 related to turbulence has been reported by the Federal Aviation Administration in 2014. Statistics reported by
28 Boeing (2015) show that fatal accidents and onboard fatalities occurred worldwide in commercial jet flights from
29 2006 through 2015. From these statistics, 23% of accidents were due to Loss of Control-In Flight (LOC-I), which is
30 the largest proportion of accidents by percentage. The International Air Transportation Association (2016) shows
31 that LOC-I frequently occurs when the aircraft speed is well below the stall speed; in conjunction with weather
32 conditions, it is the most common factor for LOC-I accidents, with 42% of LOC-I accidents having occurred under
33 degraded meteorological conditions. The Japan Transport Safety Board has identified that accidents caused by
34 turbulence accounted for 48% of aircraft accidents involving commercial airplanes from 2003-2012 in Japan. The



35 accidents caused by convective systems such as cumulonimbus have decreased owing to advances in airborne Radar
36 (Airbus, 2020; Sermi et al. 2015). However, non-cloud atmospheric turbulence, called clear air turbulence (CAT),
37 cannot be detected by Radar, as reported by Soreide et al., 2000, Barny, 2012, and Inokuchi et al., 2009; therefore,
38 airborne observation methods for CAT are needed. CAT observation and prediction systems are essential to aviation
39 safety to minimize risks of turbulence-related accidents.

40 Recently, airborne Doppler Lidar has been developed by Soreide et al., 2000; Barny, 2012; Inokuchi et al.,
41 2009; Machida, 2017; and Inokuchi and Akiyama, 2019. Lidar can detect wind velocity in clear air, but cannot work
42 during precipitation. Aerosol particles are received instead of laser beams due to a scattering light effect caused by
43 the rain particles. The aerosol particles are much smaller than precipitation droplets in the air (Inokuchi and
44 Akiyama, 2019). Japan Aerospace Exploration Agency (JAXA) is researching and developing a coherent Doppler
45 Lidar capable of remotely detecting air turbulence in clear air conditions, and has conducted the flight demonstration
46 of a Lidar system that includes a provision to provide turbulence information to pilots (Inokuchi et al., 2009,
47 Machida, 2017; Inokuchi and Akiyama, 2019). Inokuchi et al., 2009 showed that airborne Doppler Lidar can detect
48 CAT in front of an aircraft in flight at altitudes of 3,200 m during a flight observation campaign. Based on advance
49 airflow information, flight demonstrations were carried out with the aim of providing pilots with information to
50 judge the need to go around from an approach to avoid wind shear, and the need for seat belt sign lighting during
51 cruise and altitude changes (Inokuchi and Akiyama, 2019). Although Lidar systems are useful for providing wind
52 information to pilots, these systems may be able to provide short-range turbulence information to avoid turbulence
53 tactically, particularly in high altitude (Hamada, 2019) by emitting a laser beam, and by receiving scattered light
54 from aerosol particles that are much smaller than precipitation droplets in the air. Therefore, when the number of
55 aerosol particles that emit scattered light is small, it is difficult to measure wind information at a distance. As
56 altitude increases, the aerosol density decreases, and the observation range tends to decrease accordingly. The
57 maximum observation range and aerosol density measured at each altitude are shown by Inokuchi and Akiyama,
58 2019. For this reason, automatic control to alleviate aircraft vibration is important, as well as for providing
59 turbulence information.

60 The automatic control to alleviate aircraft vibration is called the gust alleviation control and has been
61 studied since the 1970s; most of them were based on feedback sensors only, such as inertial measurement units
62 (Regan and Jutte, 2012). Recently, reduced effect of turbulence by preview controlling based on airborne Lidar
63 observation has been reported in the studies by Schmitt et al., 2007; Fezans et al., 2019; and Hamada, 2019. The aim
64 of the Aircraft Wing with Advanced Technology Operation (AWIATOR) is the development of new direct-lift
65 control devices and a Lidar system for turbulence measurement (Schmitt et al., 2007). Another project on Lidar
66 systems was called “Demonstration of Lidar based CAT detection” (DELICAT) by Barny, 2012. This project
67 developed airborne ultraviolet Lidar for gust and turbulence measurements. The test flights were carried out by
68 using an Airbus 340 aircraft with ultraviolet Lidar. In both the AWIATOR and the DELICAT experiments, the
69 measurement range was short, because the Lidar was developed for controlling the aircraft automatically.

70 In order to successfully implement a gust alleviation system by using the airborne Doppler Lidar
71 technology, it is very important to measure the vertical wind velocity accurately. Both horizontal and vertical winds



72 affect the aircraft motion; the effect of changing the vertical wind velocity is greater due to the fact that the angle of
73 attack is relatively larger than the effect of changing the horizontal wind velocity, which affects only the airspeed
74 (Fezans et al., 2019). However, the single Doppler Lidar system can only detect the LOS wind as a one-dimensional
75 piece of information, and for this reason, the vertical wind velocity in front of the aircraft cannot be measured by the
76 single Lidar system (Hamada, 2019). It is necessary to perform Lidar measurements in two directions, upward and
77 downward, in order to obtain the vertical wind velocity. Figure 1 shows a representation of this concept. The vertical
78 wind velocity vector is generated from the differences between the upward and downward LOS winds by using the
79 simple vector conversion. The simple vector conversion is incapable of estimating the vertical wind velocity with
80 high accuracy to control the aircraft automatically because the technique assumes homogeneity between the upward
81 and downward Lidars (Fezans et al., 2019). In this study, a fully turbulent field with atmospheric turbulence and
82 gust was considered; under these conditions, it is difficult to estimate the vertical wind velocity with high accuracy
83 using simple vector conversion. In particular, the estimation accuracy of the vertical wind velocity rapidly worsened
84 when the estimation position was located farther ahead from the aircraft.

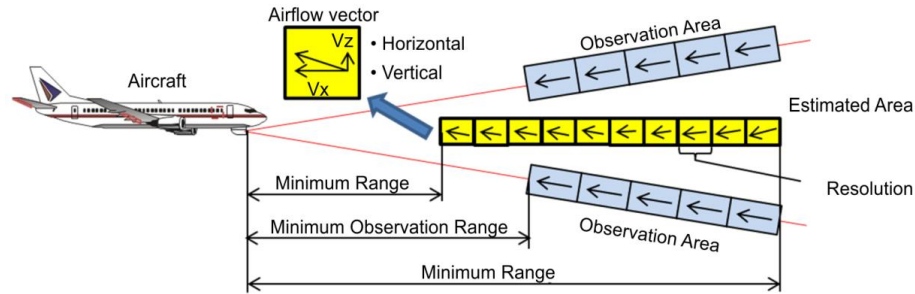
85 In addition, actual Lidar observations have some errors, noise, and loss of data, which lead to negative
86 effects on aircraft control, as reported by Misaka et al. (2015). These errors, noise and loss of data increase at higher
87 altitudes, where aerosol density is smaller than that in the atmosphere. Misaka et al. (2015) proposed a filtering
88 algorithm based on a simple Kalman filter to remove the wind velocity errors with Lidar measurements. It is
89 essential to deal with the Lidar errors, noise and loss of data more carefully for preview control. In this case, an
90 accurate airflow vector estimation method and an efficient real-time filtering algorithm are required to use Lidars
91 accurately for preview control.

92 In this study, an estimation method and an airflow vector filtering algorithm, for both horizontal and
93 vertical wind directions, based on upward and downward Lidars, is proposed for preview control to prevent
94 turbulence-induced aircraft accidents. The Lidars system in this paper is also used by JAXA in its ongoing “Lidar-
95 based gust alleviation control” research project. The Lidars are assumed to compliant with the specifications for
96 preview control currently under development by the JAXA. The proposed algorithm stores the LOS wind data
97 continuously, and uses recent and past LOS wind data to estimate the airflow vector, although the simple vector
98 conversion utilizes recent LOS wind data. The recent and past LOS wind data are used to extrapolate the wind field
99 between Lidars. The airflow vector is calculated by using the extrapolated wind data from its horizontal and vertical
100 components. The estimation accuracy of the airflow vector in front of the aircraft is improved by using the
101 extrapolated wind data because the area between the Lidars represents a more homogeneous area. A polynomial
102 expression is used to extrapolate the wind field by using the recent and past LOS wind data. In addition, the
103 proposed method can estimate the two-dimensional distribution of the wind field between the Lidars unlike the
104 simple vector conversion.

105 Two test configurations, an ideal vortex flow field and a weather field, were calculated by numerical
106 weather prediction (NWP) system, were utilized to evaluate the performance of the airflow vector. The experiment
107 generates a large amount of pseudo-Lidars measurements along flight routes from the reference wind field for



108 evaluation of the estimated performance. The experiment can compare the prediction results with the reference wind
 109 field in order to confirm the entire wind field values.



110

111

Fig. 1 Concept of the airborne Lidars observation system

112 2 Methods

113

2.1 Airborne Lidar specifications

114 The airborne Lidar observation system for preview control to prevent turbulence-induced aircraft accidents currently
 115 under development by JAXA is shown in this section. This system has airborne Lidars that are aiming upwards and
 116 downwards. The angle between airborne Lidars that are aimed in the upward and downward direction is 20 degrees,
 117 that is, 10 degrees between the horizontal line and each Lidar. Each Lidar measures the LOS wind velocity, and a
 118 couple of LOS wind velocity values are used to estimate the airflow vector in the area between the Lidars. There are
 119 additional performance requirements for preview control, namely, the estimation frequency and estimation accuracy
 120 of vertical wind velocity. The frequency of estimation is required to be more than 5 Hz, and the estimation accuracy
 121 of the vertical wind velocity is required to be lower than 2.6 ms^{-1} in the LOS distance of 500 m. In addition, the
 122 observation accuracy of LOS wind is $\pm 0.9 \text{ ms}^{-1}$ and the observation resolution of a Lidar is approximately 25 m.

123 Next, an existing technique to estimate the airflow vector, by using a couple of LOS wind values, is shown. The
 124 airflow vector in the area between upward and downward Lidars has been estimated by simple vector conversion.
 125 This procedure is a similar concept as the vertical azimuth display approach in general ground Lidar systems
 126 (Newsom et al., 2017). This simple vector conversion is given as

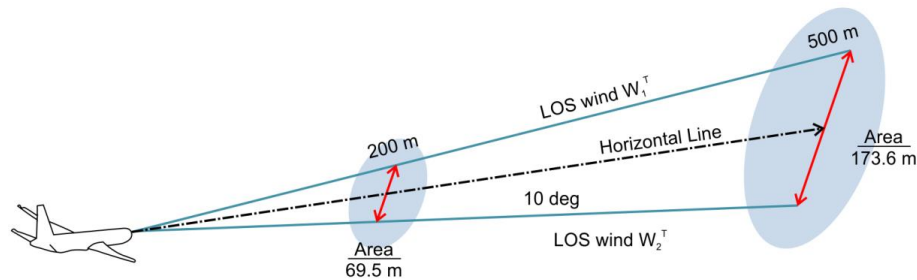
$$u_x^T = \frac{(W_1^T + W_2^T)}{2\cos\theta},$$

$$u_z^T = \frac{(W_1^T - W_2^T)}{2\sin\theta},$$
(1)

127 where u_x^T and u_z^T are the horizontal and vertical wind velocity measurements at the observation time T , W_1^T and
 128 W_2^T are the LOS wind velocities of the upward and downward directed Lidars at the observation time T , and θ is the
 129 angle between the horizontal line and each Lidar, which is 10 degrees in this study. The simple vector conversion
 130 assumes that the wind field area between the Lidars is homogeneous (Newsom et al., 2017). Figure 2 shows the
 131 explanation of the assumption. The areas between the Lidars are 69.5 m and 173.6 m at the LOS distances of 200 m



132 and 500 m ahead of the aircraft; therefore, the areas between the Lidars are assumed to be homogeneous. However,
133 the assumption of a homogeneous field would be wrong when a large fluctuation in wind velocity occurs, creating
134 turbulence. In homogenous conditions, a simple vector conversion can estimate the airflow vector accurately;
135 however, in non-homogenous conditions, the estimation is expected to have poor accuracy.



136

137

Fig. 2 The explanation of the assumption

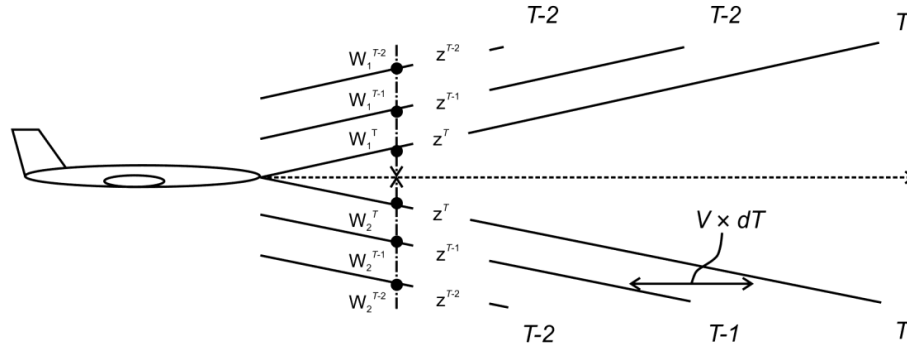
138

139

2.2 Estimation Algorithm based on Extrapolation

140 The proposed method stores the LOS wind data continuously, and uses recent and past LOS wind data values in
141 order to estimate the airflow vector, although the simple vector conversion utilizes recent LOS wind data. The recent
142 and past LOS wind data are used to extrapolate the wind field between the Lidars, and this area between the Lidars
143 has not been measured directly by the Lidars. The airflow vector is calculated by using Eq. (1) and the extrapolated
144 wind data of its horizontal and vertical components. The airflow vector estimation accuracy far ahead of the aircraft
145 is improved by using the extrapolated wind data because it is valid to assume that the area between upward and
146 downward Lidars is non-homogeneous. The simple vector conversion only can be applied to homogenous wind field
147 conditions, but the algorithm can extrapolate data points by using past measurements so that it can be used in non-
148 homogenous wind field conditions. A polynomial expression is used to extrapolate the wind field values by using
149 the recent and past LOS wind data. In addition, the proposed method can estimate the two-dimensional distribution
150 of the wind field between the Lidars unlike the simple vector conversion.

151 Figure 3 shows the overview of the proposed method estimation method when an actual data point and two-past
152 LOS wind data points are used. When the aircraft speed is V and the time span of observation is dt , the airflow
153 moves backwards at $V \times dt$ because the aircraft is advancing. Actual observation times are denoted as T and past
154 observation times are $T-1$ and $T-2$. The proposed method uses the actual LOS wind values (W_1^T and W_2^T) and the
155 past LOS wind values (W_1^{T-1} , W_2^{T-1} and W_1^{T-2} , W_2^{T-2}). The distances between the horizontal line and each Lidar are
156 denoted as z^T , z^{T-1} and z^{T-2} , respectively. A first-degree polynomial expression of the least-squares method (LSM) is
157 applied and using some LOS wind data values, the wind field values are extrapolated according to Eqs. (2) and (3).
158 The calculated polynomial expression is used to obtain the extrapolated LOS wind at the horizontal line, and the
159 airflow vector is calculated by Eq. (1) and the extrapolated LOS wind.



160
 161
 162

Fig. 3 Overview of estimation by proposed method when the recent and two-past LOS wind data are used

$$W_j'(z) = a_j z + b_j \quad (2)$$

$$a_j = \frac{N \sum_{i=T-(N-1)}^T z^i W_j^i - \sum_{i=T-(N-1)}^T z^i \sum_{i=T-(N-1)}^T W_j^i}{N \sum_{i=T-(N-1)}^T (z^i)^2 - \left(\sum_{i=T-(N-1)}^T z^i \right)^2}, \quad (3)$$

$$b_j = \frac{\sum_{i=T-(N-1)}^T z^i \sum_{i=T-(N-1)}^T W_j^i - \sum_{i=T-(N-1)}^T z^i W_j^i \sum_{i=T-(N-1)}^T z^i}{N \sum_{i=T-(N-1)}^T (z^i)^2 - \left(\sum_{i=T-(N-1)}^T z^i \right)^2}.$$

163

164

2.3 Filtering error and the lack of wind velocity data

165

166

167

168

169

170

171

172

173

174

In this study, two filtering algorithms are used to remove the error and the loss of data of LOS wind velocity in airborne Lidars. Firstly, we use a filtering algorithm that is a simple representation of the Kalman filter with simplified Kalman gain (Misaka et al., 2015). The algorithm assumes that infinite variance is used to exclude outliers and loss of data. This method uses the Lidar spectrum data at each range-bin, and the algorithm defines the validity of the measurements during the Lidar data peak detection process. To identify the correct and non-correct LOS wind velocity values, two spectrum thresholds are defined. Firstly, the largest and second-largest spectrum values, k_{1st} and k_{2nd} , are adjacent to each other, i.e., the distance between the largest and second-largest spectrum values in the Fast Fourier Transform is equal to one. Secondly, the distance from the averaged spectrum peak k_{ave} is less than a certain allowance k_{dif} , which represents the only hyper-parameter in this algorithm as well as a parameter related to smoothness. In this study, the filtering algorithm is carried out first when the observation data is obtained.

$$K_{i,j} = \begin{cases} 1 & |k_{1st} - k_{2nd}| = 1 \text{ and } |k_{1st} - k_{ave}| < k_{dif} \\ 0 & \text{Others} \end{cases} \quad (4)$$



175 Secondly, a robust LSM estimation, based on Tuckey’s biweight methodology (Huber, 2008), is carried out
 176 to reduce the impact of the error in the LOS wind velocity. This method is based on the LOS wind data unlike the
 177 spectrum data of Lidar observation at the first method. Although the filtering algorithm based on a simple Kalman
 178 filter can remove the error, it is essential to deal with the error and the loss of data of the Lidars more carefully when
 179 the filtering algorithm is used for the preview control. Therefore, the robustness of the estimated airflow vector is
 180 secured by using the filtering algorithm based on a simple Kalman filter together with robust LSM. In addition, the
 181 robust LSM estimation can make use of the extrapolation algorithm effectively as per Eqs. (2) and (3). Therefore,
 182 the robust LSM estimation provides a simpler and more robust algorithm. The concept of a robust LSM is validated
 183 by analyzing the difference between the observed LOS wind values and those LOS wind values estimated by the
 184 polynomial expression. Weights are defined to each LOS wind velocity value, and the weights are changed
 185 depending on the validation numbers. The difference d_j^T between the observed LOS wind values and estimated LOS
 186 wind values from the polynomial expression is defined by Eq. (5) with Eq. (2). The permissible difference range L is
 187 defined and the weights $w_j^T (d_j^T)$ are calculated depending on d_j^T . Three thresholds for defining $w_j^T (d_j^T)$ from L are
 188 used as shown in Eq. (6). Equation 7 shows the calculation of the polynomial expression of the first degree with
 189 LSM and weights $w_j^T (d_j^T)$.

$$d_j^T = W_j^T - (a_j z + b_j) \quad (5)$$

$$w_j^T (d_j^T) = 0 \quad (d_j^T < -L)$$

$$w_j^T (d_j^T) = \left(1 - \left(\frac{d_j^T}{w_j^T} \right)^2 \right) \quad (-L \leq d_j^T \leq L) \quad (6)$$

$$w_j^T (d_j^T) = 0 \quad (d_j^T > L)$$

$$a_j' = \frac{\sum_{i=T-(N-1)}^T w_j^i \sum_{i=T-(N-1)}^T w_j^i z^i W_j^i - \sum_{i=T-(N-1)}^T w_j^i z^i \sum_{i=T-(N-1)}^T w_j^i W_j^i}{\sum_{i=T-(N-1)}^T w_j^i \sum_{i=T-(N-1)}^T w_j^i (z^i)^2 - \left(\sum_{i=T-(N-1)}^T w_j^i z^i \right)^2} \quad (7)$$

$$b_j' = \frac{\sum_{i=T-(N-1)}^T w_j^i z^i \sum_{i=T-(N-1)}^T w_j^i W_j^i - \sum_{i=T-(N-1)}^T w_j^i z^i W_j^i \sum_{i=T-(N-1)}^T w_j^i z^i}{\sum_{i=T-(N-1)}^T w_j^i \sum_{i=T-(N-1)}^T w_j^i (z^i)^2 - \left(\sum_{i=T-(N-1)}^T w_j^i z^i \right)^2}$$

190

191 2.4 Filtering wind velocity noise

192 The Lidar observation is subject to not only measuring errors and loss of LOS data values but also random
 193 noise; this type of noise also leads to a poor estimation of the airflow vector. A simple spline algorithm generates a
 194 curve that passes through all sample points; therefore, the simple spline algorithm is not able to generate a smooth
 195 curve when the sample points have random noise, and a smoothing spline algorithm is applied to remove the random
 196 noise of the Lidar LOS wind values, as in the study by Woltring, 1986. The generated smoothing spline algorithm



197 curve does not pass through all sample points, and because of that, it can produce a smoother curve, even if it has
198 random noise from Lidar LOS wind measurements. The smoothing spline model minimizes the criterion function C_p ,
199 per Eq. (8) where y_i is a sample point value, $s_p(x)$ is the value generated by a simple spline algorithm, v_i is a
200 weighted factor and p is regularization parameter. The smoothest curve is generated when the criterion function C_p
201 is minimized.

$$C_p = \sum_{i=1}^n v_i \{y_i - s_p(x)\}^2 + p \int \left(\frac{d^2 s_p}{dx^2} \right)^2 dx \quad (8)$$

202 **2.5 System flowchart**

203 The airflow vector estimation algorithm is a sequence of five different processes, which are summarized
204 below. The system flowchart is shown in Fig. 4.

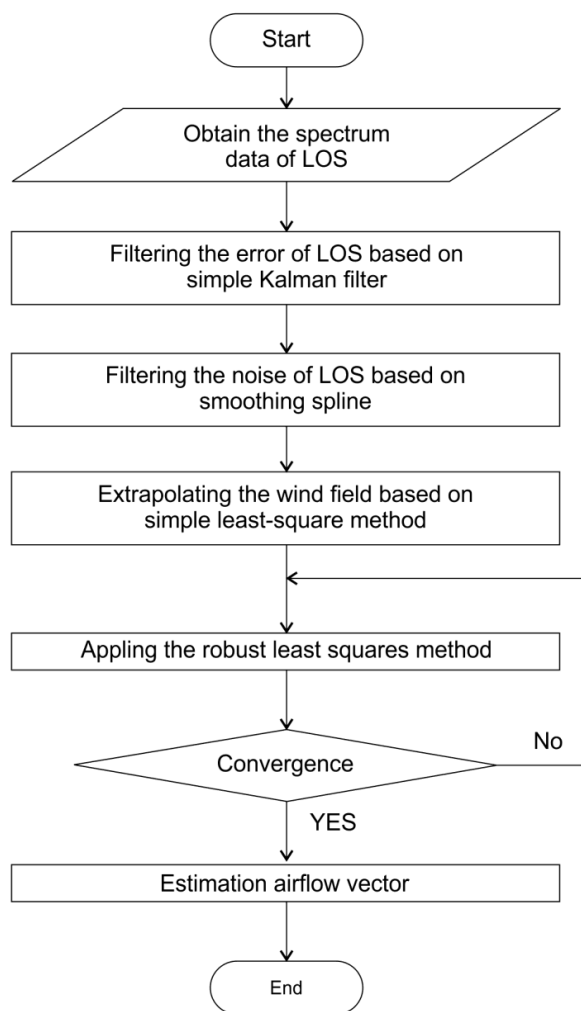
205 1) The filtering algorithm based on simple Kalman filter is carried out to remove the error of LOS
206 wind data when the Lidar measures LOS wind data values.

207 2) The smoothing spline method is applied to reduce the negative effect of the random noise of LOS
208 wind data values and extrapolates the value at the position for which no measurements can be read. . This is
209 identified as the first step error.

210 3) The extrapolation, based on the polynomial expression, is carried out to estimate the wind field
211 values by using current and past LOS wind data.

212 4) A robust LSM model is applied to obtain a more accurate polynomial expression, and repeats the
213 calculation until the parameter converges.

214 5) The airflow vector is calculated by Eq. (1) and the extrapolated LOS wind.



215

216

Fig. 4 System flowchart for the airflow vector estimation algorithm

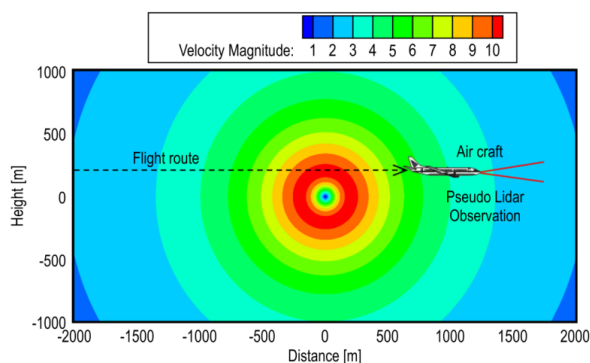
217 3 Test Configurations

218 3.1 Ideal vortex model

219 Numerical experiments are used to evaluate the performance of actual airborne Lidars. The ideal vortex model is
220 defined and used to evaluate the estimated performance of the airflow vector. In this study, the Hallock-Burnham
221 vortex model (Hinton et al., 1997) is used as the ideal vortex model. The experiment generates a large amount of
222 pseudo Lidars values along flight routes by the ideal vortex model. The airflow vector is estimated by using the
223 pseudo-Lidars readings, and the estimated airflow vector is compared with the reference field of the ideal vortex
224 model. The experiment can compare the estimation results with the reference wind field values to confirm the entire



225 wind field. Figure 5 shows the distribution of vertical wind velocity generated by the Hallock-Burnham vortex
226 model.



227

228

Fig. 5 The distribution of vertical wind velocity generated by the vortex model

229

230

3.2 NWP model

231

232

233

234

235

236

237

238

239

240

241

242

243

244

The results predicted by the numerical weather model, that is, the Japan Meteorological Agency Non-Hydrostatic Model (JMA-NHM), are used to evaluate the airflow vector estimation performance. In this study, JMA-NHM is employed to obtain the wind field for the evaluation (Saito et al., 2007 and Kikuchi et al., 2015). To obtain the high-resolution weather prediction, a one-way multi-nesting technique (Kikuchi et al. 2015) is conducted for downscaling purposes. The computational domain is nested four times to increase grid resolutions from 5.0 to 0.05 km gradually (as follows: 5.0, 1.5, 0.5, 0.15, and 0.05 km).

A three-hour mesoscale objective analysis data, collected using a mesoscale four-dimensional variational data assimilation system at the Japan Meteorological Agency (Saito et al., 2007), are used for the initial condition of 5.0-km grid resolution. The experiment used the JMA-NHM wind field, which can provide more realistic test results than the ideal vortex model for the performance evaluation. The experiment generates a large amount of pseudo twin Lidar observation values along flight routes from the wind field data generated by JMA-NHM. The airflow vector is estimated by using the pseudo-Lidar observation, and the estimated airflow vector is compared with the reference field of JMA-NHM. Figures 6 and 7 show the experiment concept used by JMA-NHM and the distribution of the vertical wind velocity values generated by JMA-NHM.

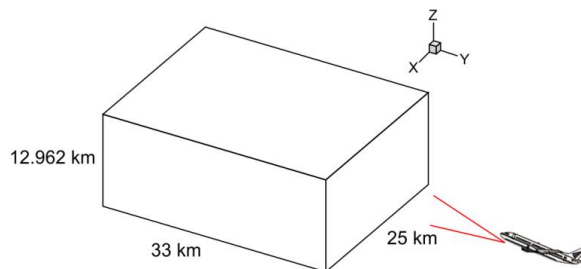




Fig. 6 The concept of the experiment used by JMA-NHM.

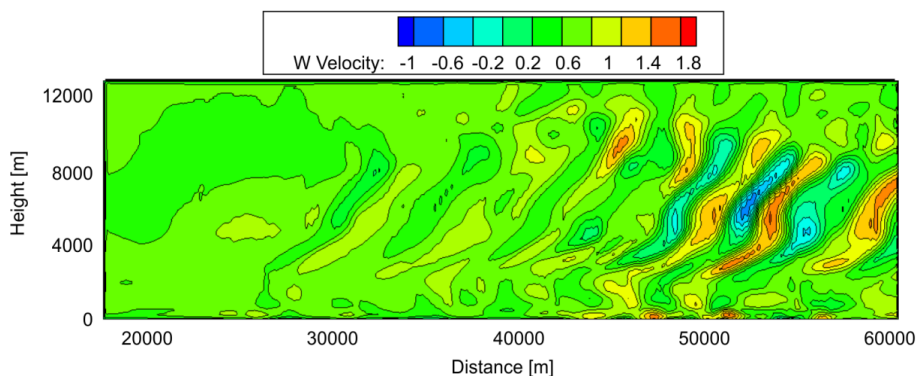


Fig. 7 Vertical wind velocity distribution map generated by JMA-NHM

245

246

247

3.3 Generation of pseudo errors and noise

248 Errors and noise were generated artificially to confirm the effect of the proposed filtering algorithms. Errors and
 249 noise are generated by using the parameter of the backscattering coefficient in the atmosphere and the statistics-
 250 based coherent Lidar equation (Kameyama et al., 2007). The backscattering coefficient that is strongly related to the
 251 aerosol density in the atmosphere has an impact on the Lidar measurements and estimation performance. When the
 252 backscattering coefficient is very low, the measurement performance is worse, and the LOS wind data show errors
 253 and noise. In addition, the measurement performance is related to the focal distance, pulse width and Lidar power
 254 (Kameyama et al., 2007). The signal-noise ratio (SNR) at the receiver, at each LOS distance, is calculated by using
 255 the coherent Lidar equation and the detailed operating condition of JAXA's Lidar [7-9].

$$SNR(R) = \frac{\eta P_t \Delta R \beta K^2 R \frac{\pi D^2}{4R^2}}{h f B SRF(R)} \quad (9)$$

$$SRF(R) = 1 + \left\{1 - \frac{R}{F}\right\}^2 \left\{\frac{k(A_c D)^2}{8R}\right\}^2 + \left\{\frac{A_c D}{2S_o(R)}\right\}^2 \quad (10)$$

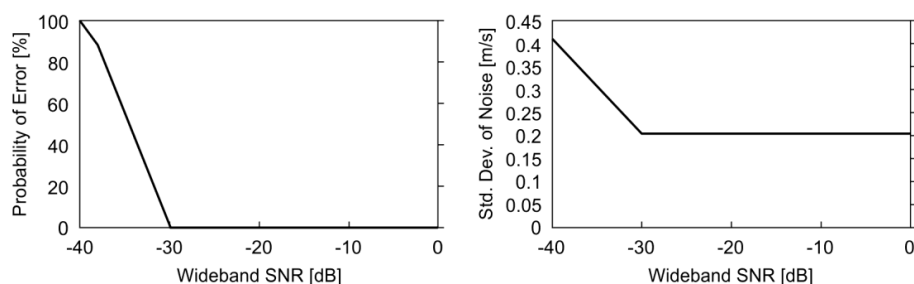
$$S_o(R) = (1.1 k^2 R C_n^2)^{-\frac{3}{5}} \quad (11)$$

256

257 R is the observation distance, η is system efficiency, P_t is light transmission power, ΔR is the resolution range, β is
 258 backscattering coefficient, K is atmospheric transmittance, D is the opening size of optical antenna, h is Planck
 259 constant, f is optical frequency, B is received bandwidth, F is focal distance, k is wave number, A_c is vignetting
 260 factor of optical antenna and C_n^2 is atmospheric structure constant. In this study, the conditions are set according to
 261 the design specification for airborne Lidars. In this study, six atmospheric conditions are prepared in order to
 262 evaluate the filtering performance. The backscattering coefficients are (Standard case) $1.8 \times 10^{-8} \text{ sr}^{-1} \text{ m}^{-1}$, (a) 1.8×10^{-11}



263 $\text{sr}^{-1}\text{m}^{-1}$, (b) $1.35 \times 10^{-11} \text{sr}^{-1}\text{m}^{-1}$, (c) $0.9 \times 10^{-11} \text{sr}^{-1}\text{m}^{-1}$, (d) $0.45 \times 10^{-11} \text{sr}^{-1}\text{m}^{-1}$, and (e) $0.18 \times 10^{-11} \text{sr}^{-1}\text{m}^{-1}$. Figure 8 shows
264 the statistics for the error and noise depending on the SNR bandwidth.



265
266

Fig. 8 Probability of error and standard deviation of noise

267 **4 Results**

268 **4.1 Ideal Vortex Model without Error and Noise**

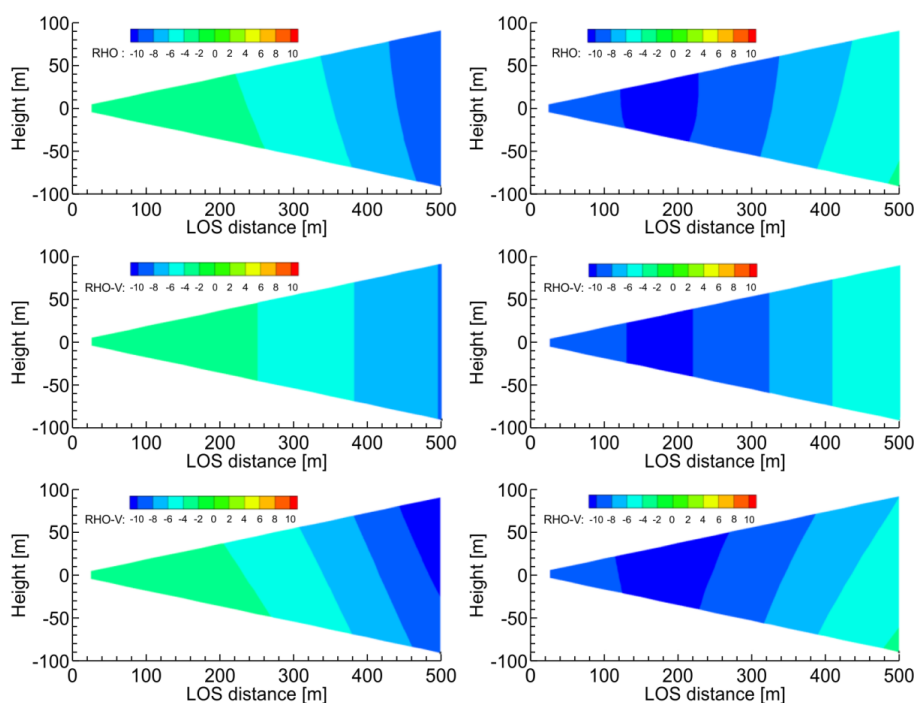
269 The numerical experiments of the ideal vortex model are carried out, and Figs. 9 and 10 show the distributions of the
270 horizontal and vertical wind components that are estimated by the simple vector conversion and the proposed
271 method. The upper figures show the wind field values generated by the ideal vortex model; the middle figures
272 represent the wind field values estimated by the simple vector conversion method, and the lower figures are the wind
273 field values estimated by the proposed method with five-past LOS wind datasets. Figures to the left represent the
274 horizontal wind values, and figures to the right represent the vertical wind values. Figure 9 shows the results after 10
275 s and Fig. 10 after 15 s.

276 As shown in Figs. 9 and 10, the results of the simple vector conversion method cannot be shown in a two-
277 dimensional distribution between the Lidars, as the assumption is that the wind field of the area between the Lidars
278 is homogeneous. On the other hand, it is confirmed that the proposed method can estimate the two-dimensional
279 distribution of wind field values between the Lidars. Figure 9 shows that the two-dimensional distribution obtained
280 with the proposed method are very similar to that of the reference field. In addition, the results show that the
281 horizontal wind velocity with the simple vector conversion is approximately -7 m/s , whereas that with the proposed
282 method is -9.5 ms^{-1} ; the horizontal wind velocity of the reference field is -9.0 ms^{-1} at LOS distance of 450-500 m.
283 Figure 10 shows that the results of the horizontal wind and vertical wind with simple vector conversion are
284 considerably lower than those of the reference field. The horizontal wind results show that the value obtained with
285 the simple vector conversion is approximately -9.5 ms^{-1} , whereas that with the proposed method is approximately -3.5 ms^{-1} ;
286 the horizontal wind velocity of the reference field is approximately -4.5 ms^{-1} at LOS distance of 450-500 m.
287 The vertical wind results show that the value obtained with simple vector conversion is approximately -1.0 m/s ,
288 whereas that obtained with the proposed method is approximately 8.5 ms^{-1} ; the vertical wind velocity of the
289 reference field is approximately 7.0 ms^{-1} at LOS distance of 450-500 m. Therefore, simple vector conversion has
290 significantly large errors between the reference and estimated values. The errors in both the horizontal and vertical
291 wind values estimated by the proposed method are much smaller than those estimated with simple vector conversion.



292 Although the two-dimensional distribution of the horizontal wind field values of the proposed method is larger than
293 that of the reference field at LOS distance of 450-500 m, the two-dimensional distribution of the vertical wind field
294 values of the proposed method can provide a good assessment of the reference field shown in Fig. 10. The 15-s
295 timing in Fig. 10 is a more challenging case than others because the aircraft is positioned very close to the center of
296 the vortex, and the wind direction changes abruptly. Although it is difficult to estimate the perfect wind field value
297 at this time by using the proposed method, it is confirmed that the proposed estimation method has much higher
298 accuracy than simple vector conversion. From the above, the proposed method has much better performance than
299 the simple vector conversion method, and it can estimate the two-dimensional distribution of wind field values
300 accurately unlike the simple vector conversion method.

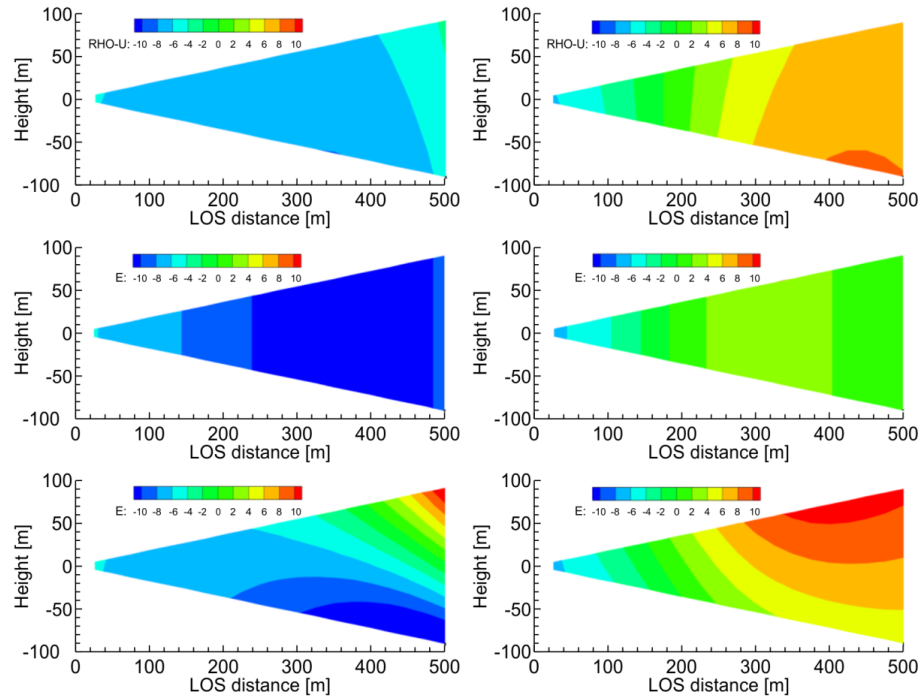
301 Next, a statistical estimation performance is conducted by using 100-pseudo routes; Fig. 11 shows the results for the
302 vertical wind values along with the performance demand for automatic control. The root mean square error (RMSE)
303 between the reference field value and the estimated wind field value is used for evaluating the estimation
304 performance. In addition, the difference in the number of past Lidar observations used to determine the wind field,
305 that is the past LOS wind, is checked. The simple vector conversion cannot satisfy the performance demand at LOS
306 distance farther than 350 m. This means that it might be difficult to achieve preview control using the simple vector
307 conversion method. At the LOS distance of 500 m, the RMSEs of the vertical wind values of the simple vector
308 conversion and proposed method is approximately 4.0 ms^{-1} and 1.2 ms^{-1} , respectively, and the RMSE can be reduced
309 to 30%. The proposed method can satisfy the performance demand even if the number of using the past LOS wind
310 values is different. In this case, a lower number of using the past LOS wind leads to better estimation performance.



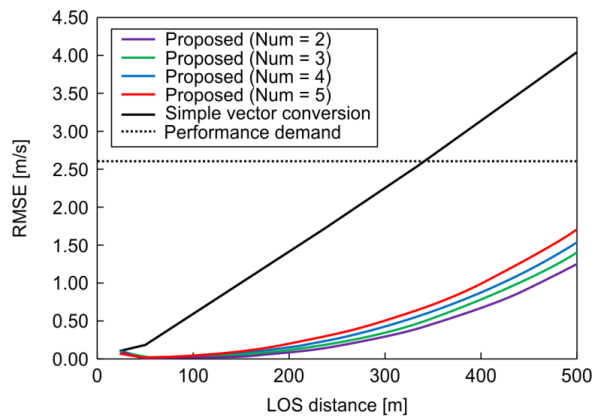
311



312 **Fig. 9** Distributions of the horizontal and vertical wind components estimated by the simple vector conversion method
 313 vs. the proposed method (10 s)



314 **Fig. 10** Distributions of the horizontal and vertical wind components estimated by the simple vector conversion method
 315 vs. the proposed method (15 s)
 316



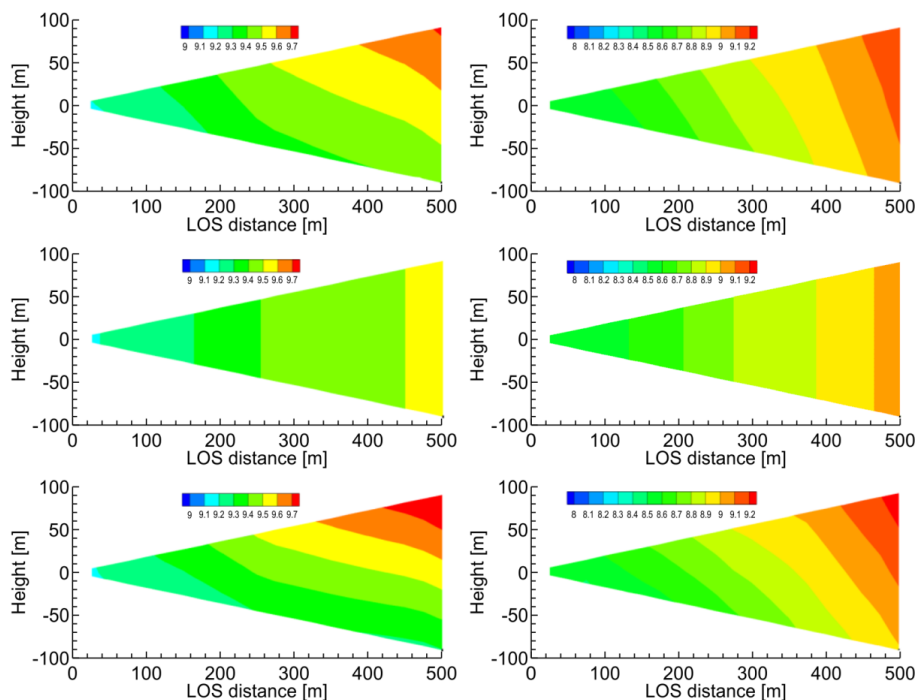
317 **Fig. 11** Statistical estimation performance of vertical wind values (Ideal vortex model)
 318

319 **4.1 NWP without Error and Noise**

320 The numerical experiments with NWP values were carried out, and Figs. 12 and 13 show the distributions of the
 321 horizontal and vertical wind components that are estimated by the simple vector conversion and the proposed
 322 method. Upper figures are reference wind field values generated by NWP; middle figures are the wind fields

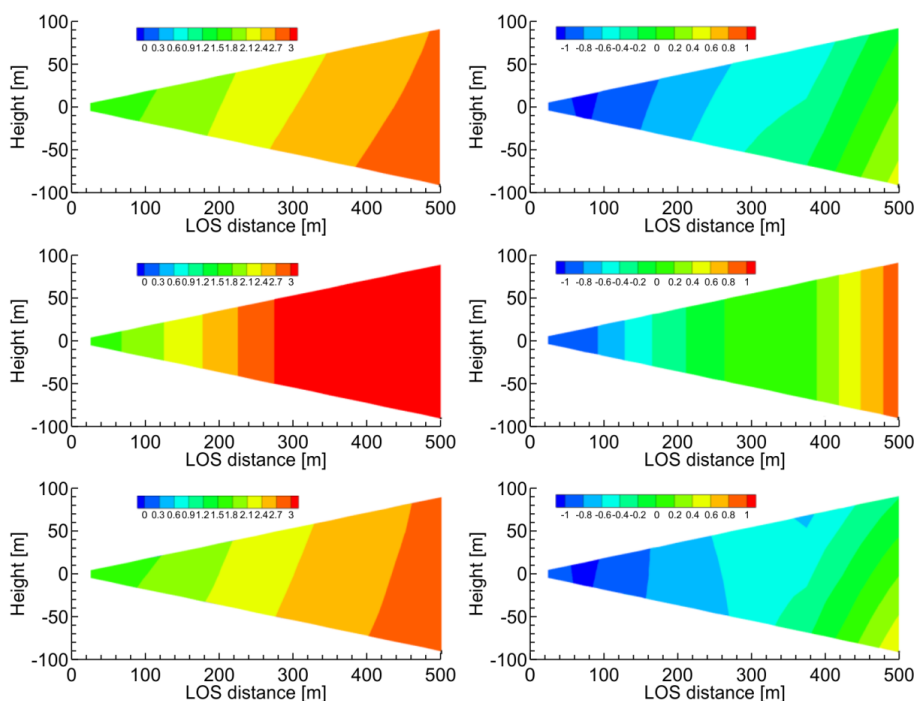


323 estimated by the simple vector conversion method; lower figures are the wind fields estimated by the proposed
324 method with five-past LOS wind. Left figures correspond to horizontal wind, and right figures correspond to vertical
325 wind. Figure 12 shows the results after 10 s and Fig. 13 after 15 s. As shown in Figs. 12 and 13, the results of the
326 simple vector conversion method cannot show the two-dimensional distribution of the wind field between the Lidars.
327 On the other hand, the proposed method can estimate the two-dimensional distribution of the wind field between the
328 Lidars. Figure 13 shows that the wind velocity of the simple vector conversion method is higher than the reference
329 fields at 300-500 m of LOS distance. From the above, the proposed method has much better performance than
330 simple vector conversions.
331 Next, the statistical estimation performance is conducted by using 100-pseudo routes, and Fig. 14 shows the results
332 of the statistical estimation performance with the performance demand to control automatically. In addition, the
333 difference of the number of using past LOS wind is also checked. In this case, both simple vector conversion and the
334 proposed method can satisfy the performance demand to preview control; however, the simple vector conversion
335 performance results are much worse than those of the proposed method. The proposed method can estimate quite
336 accurate wind field values. In this case, the use of past LOS wind numbers, higher leads to a better estimation
337 performance.

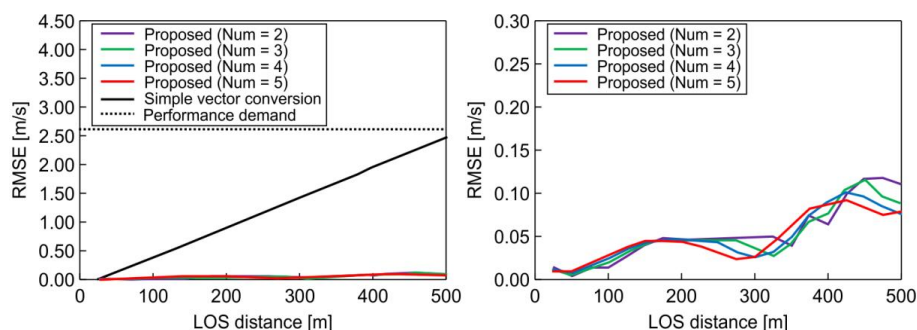


338

339 **Fig. 12 Distributions of the horizontal and vertical wind components that are estimated by simple vector conversion and**
340 **the proposed method (10 s)**



341
 342 **Fig. 13 Distributions of the horizontal and vertical wind components that are estimated by simple vector conversion**
 343 **and the proposed method (15 s)**



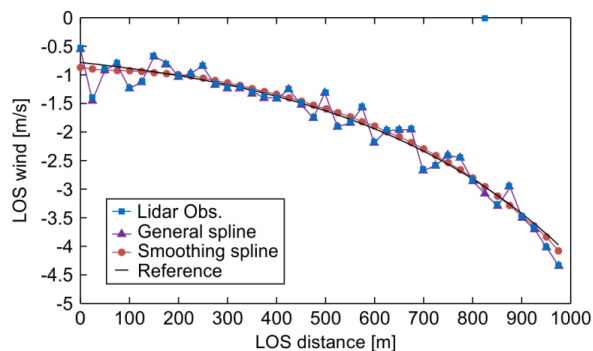
344
 345 **Fig. 14 Statistical estimation performance (NWP) results**

346 **4.2 Ideal vortex model with error and noise**

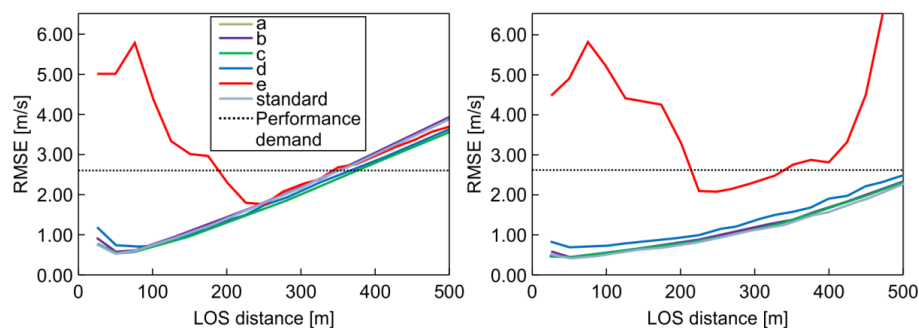
347 In this section, the numerical experiments with error and noise of LOS wind values are conducted to evaluate the
 348 estimation performance of the proposed method. This numerical experiment shows the error/noise-filtering
 349 performance difference between simple vector conversion and the proposed method with extrapolation by using the
 350 past LOS wind. In this study, the atmospheric conditions are used to evaluate six different cases, to generate error
 351 and noise data in the LOS wind values. In this study, six atmospheric conditions are prepared in order to evaluate the
 352 filtering performance. The backscattering coefficients are (Standard case) $1.8 \times 10^{-8} \text{ sr}^{-1} \text{ m}^{-1}$, (a) $1.8 \times 10^{-11} \text{ sr}^{-1} \text{ m}^{-1}$, (b)
 353 $1.35 \times 10^{-11} \text{ sr}^{-1} \text{ m}^{-1}$, (c) $0.9 \times 10^{-11} \text{ sr}^{-1} \text{ m}^{-1}$, (d) $0.45 \times 10^{-11} \text{ sr}^{-1} \text{ m}^{-1}$, and (e) $0.18 \times 10^{-11} \text{ sr}^{-1} \text{ m}^{-1}$.



354 The numerical experiments with the ideal vortex model were carried out. Figure 15 shows the LOS wind values,
 355 which include the measured data with error and noise, reference wind, the smoothing spline, and the general spline
 356 model results. Figure 15 shows that the smoothing spline can filter the error and noise data of LOS wind values.
 357 When the general spline is used, the error can be filtered correctly by using a simple Kalman filter and a robust
 358 LSM; however, the noise cannot be filtered. Next, a statistical estimation performance is conducted by using 100-
 359 pseudo routes, and Fig. 16 shows the results of the statistical estimation performance with error and noise. In
 360 addition, the difference of the atmospheric condition in six-case (standard, (a), (b), (c), (d), (e) in the backscattering
 361 coefficients) is also checked. The figure to the left is the simple vector conversion results, and the figure to the right
 362 shows the proposed method results. The simple vector conversion cannot satisfy the performance demand at a
 363 distance farther than 350 m LOS, and cannot work correctly at atmospheric condition (e). The proposed method can
 364 satisfy the performance demand except at atmospheric conditions (e). The proposed method shows much better
 365 performance than the simple vector conversion, even though it is difficult to estimate the wind field values for
 366 atmospheric condition (e) by using both the simple vector conversion and the proposed method, due to the fact, that
 367 atmospheric condition (e) contains much larger noise levels than other conditions.



368
 369 **Fig. 15 LOS wind values with measured data with error and noise, reference wind, the smoothing spline and general**
 370 **spline**

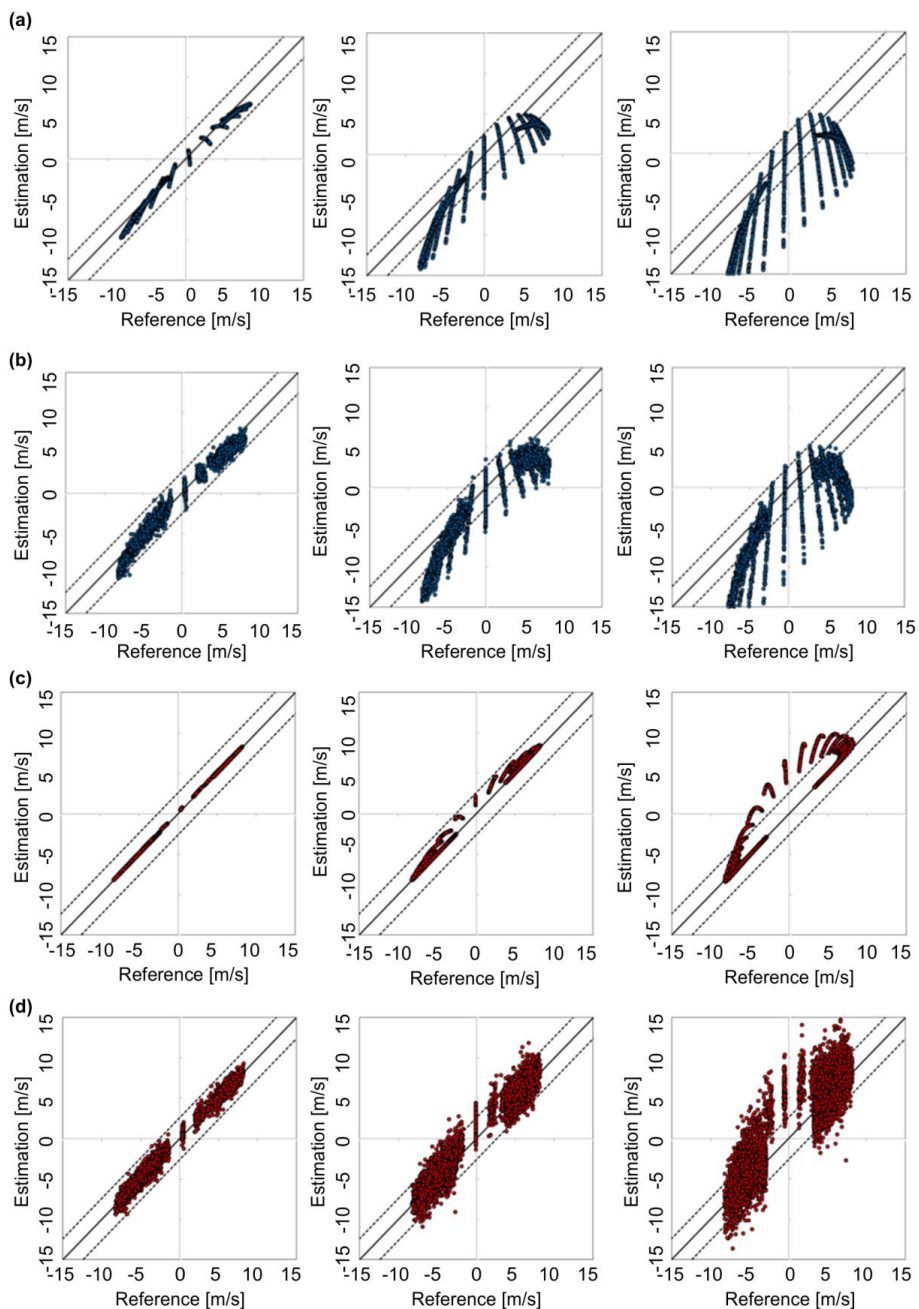


371
 372 **Fig. 16 Statistical estimation performance results with the error and noise (Ideal vortex model)**

373 In addition, the cross-plots of the reference and the estimated vertical wind are shown as Fig. 17. In Fig. 17 (a), (b)
 374 the results of the simple vector conversion are presented, (c), (d) show the results of the proposed method, (a) and
 375 (c) are the cases without error and noise, and the (b) and (d) are the cases with error and noise. The left figures are



376 the wind data at 100 m LOS distance, middle figures are the wind data at 300 m LOS distance, and the right figures
377 are the wind data at 500 m LOS distance. The dots indicate the wind speed estimated at 5 Hz, and the dotted lines
378 indicate the performance demand of the control. By comparing (a) and (c), we can deduct that the proposed method
379 provides a much better estimation than the simple vector conversion. The results in (b) and (d) are spread wider than
380 those in (a) and (c), because of the noise data of LOS wind values. It is worth mentioning that the noise data have
381 more negative effects on the result at 500-m LOS distance than at 100 m and 300 m LOS. A comparison of (b) and
382 (d) shows that the proposed method can provide more accurate estimations than the simple vector conversion
383 method.



384

385

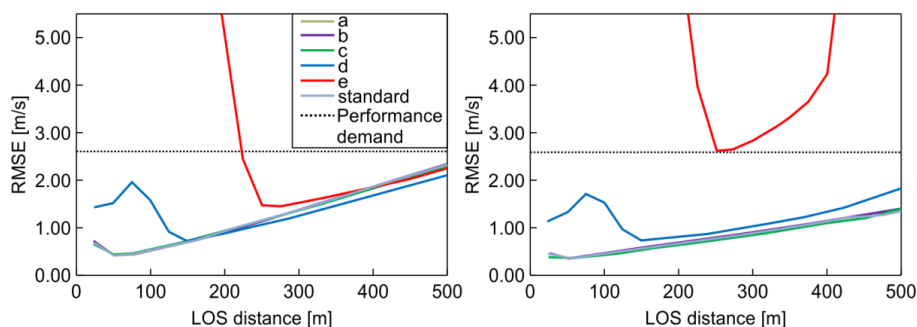
386

Fig. 17 Cross-plots of the reference and the estimated vertical wind



387 4.3 NWP with error and noise

388 The numerical experiments with NWP were carried out. The statistical estimation performance is conducted by
389 using 100-pseudo routes, and Fig. 18 shows the results of the statistical estimation performance with error and noise.
390 In addition, six different atmospheric condition cases (standard, (a), (b), (c), (d), and (e) in the backscattering
391 coefficients) were used. Figures to the left show simple vector conversion results and figures to the right show
392 results with the proposed method. In this case, both the simple vector conversion and the proposed method can
393 satisfy the performance demand to preview control; however, the simple vector conversion shows worse
394 performance compared to the proposed method. The proposed method can estimate quite accurately wind field
395 values. In addition, the proposed method displays better performance than the simple vector conversion method, and
396 similar to the previous experiment, it is difficult to estimate the wind field values for atmospheric condition (e) by
397 using both the simple vector conversion and the proposed method.



398
399
400

Fig. 18 The results of the statistical estimation performance with the error and noise (NWP)

401 5. Conclusion

402 In this study, an airflow vector estimation algorithm based on upward and downward airborne Lidars has been
403 proposed for preview control to prevent turbulence-induced aircraft accidents. This estimation algorithm uses the
404 technique of extrapolating the wind field values by using the LSM and the current and past LOS wind datasets to
405 improve the accuracy of estimated wind values. Two test configurations of numerical experiments, 1) ideal vortex
406 flow field and 2) realistic weather field values with calculated NWP numbers, were used to evaluate the estimated
407 performance of the airflow vector.

408 The numerical experiments of LOS wind were conducted to evaluate the estimation performance of the proposed
409 method. These numerical experiments showed the difference in performance between simple vector conversion
410 methods and the proposed extrapolation method. The proposed method has much better performance than the simple
411 vector conversion methods, and it can estimate the two-dimensional distribution of wind field values accurately,
412 unlike the simple vector conversion method. The estimation performance and the computational cost of the proposed
413 method can satisfy the performance demand for preview control.



414 The numerical experiments with error and noise of LOS wind were conducted to evaluate the performance of the
415 proposed estimation method. These numerical experiments showed the error/noise-filtering performance difference
416 between the simple vector conversion method and the proposed extrapolation method. It was also shown that the
417 smoothing spline model could filter noise correctly and reduce its negative effects. Therefore, the proposed method
418 has shown a much better performance than the simple vector conversion method; however, it is still difficult to
419 estimate the wind field values for atmospheric condition (e) with both methods. Atmospheric condition (e) has larger
420 noise than other conditions, and when the noise exceeds a certain level, it is difficult to estimate the airflow
421 regardless of the method applied.

422 The findings of this study are subject to certain limitations. The target size of the atmospheric turbulence by the
423 proposed algorithm is assumed to be comparable or larger than the observation area between the Lidars. Therefore,
424 it is difficult to estimate a wind field with turbulence smaller than that of the observation area between the Lidars.
425 However, the effect on the aircraft vibration due to such minor turbulence is minimal, and it is considered to be
426 excluded from the proposed algorithm. The second limitation is that the current results are obtained from numerical
427 experiments and not from evaluations of actual observations. Currently, the LIDAR system is being modified to be
428 smaller and lighter in order to suit small experimental aircraft. Flight demonstrations are to be performed in 2021.
429 The results of this research will be applied to this flight demonstration.

430

431 The proposed algorithm can satisfy the performance demands for preview control in both estimation performance
432 and computational cost. The proposed method can estimate a two-dimensional distribution that cannot be estimated
433 by existing methods. This is valuable information for improving the accuracy of the preview control: for example, it
434 is now possible to cope with a critical case where the flight direction of the aircraft is at a steep angle with the
435 aircraft either ascending or descending. This point is also an advantage of the proposed method.

436 **Author Contributions**

437 Ryota Kikuchi, Takashi Misaka, and Shigeru Obayashi designed the experiments and Ryota Kikuchi
438 performed the experiments, developed the model code, performed the simulations, and prepared the manuscript with
439 contributions from all co-authors. Hamaki Inokuchi contributed to the analysis and interpretation of data related to
440 Lidar, and assisted in the preparation of the manuscript. All authors approve the final version of the manuscript, and
441 agree to be accountable for all aspects of the work in ensuring that questions related to the accuracy or integrity of
442 any part of the work are appropriately investigated and resolved.

443 **Competing Interests**

444 The authors declare that they have no conflict of interest.



445 **References**

- 446 Airbus, Flight Operations Briefing Notes Adverse Weather Operations Optimum Use of the Weather Radar,
447 available at: <https://safetyfirst.airbus.com/optimum-use-of-weather-radar/>, 2020.
- 448 Barny, H.: DELICAT - Demonstration of LIdar based Clear Air Turbulence detection, Innovation for Sustainable
449 Aviation in a Global Environment, in: Proceedings of the Sixth European Aeronautics Days, 253, 2012.
- 450 Boeing: Statistical Summary of Commercial Jet Airplane Accidents, 2015.
- 451 Federal Aviation Administration, Preventing injuries caused by turbulence 2006, available at:
452 https://www.faa.gov/regulations_policies/advisory_circulars/index.cfm/go/document/information/documentid/99831,
453 2020.
- 454 Fezans, N., Joos, H.D., and Deiler, C.: Gust load alleviation for a long-range aircraft with and without anticipation,
455 CEAS Aeronautical Journal, 2019, 1-25.
- 456 Hamada, Y.: New LMI-based conditions for preview feedforward synthesis, Control Engineering Practice, 90, 19-26,
457 2019
- 458 Hinton, D. A., and Tatnall, C. R.: A candidate wake vortex strength definition for application to the NASA aircraft
459 vortex spacing system (AVOSS), NASA Technical Reports, 1997.
- 460 Huber, P. J.: Robust Statistics, Springer, Berlin, Heidelberg, 2008.
- 461 Inokuchi, H., Tanaka, H., and Ando, T.: Development of an onboard doppler lidar for flight safety, Journal of
462 aircraft, 46.4, 1411-1415, 2009
- 463 Inokuchi, H., and Akiyama, T.: Flight Demonstration of an Airborne Coherent Doppler Lidar, Asia Pacific
464 International Symposium on Aerospace Technology, 2019.
- 465 International Air Transportation Association, Safety Report 2015, 2016.
- 466 Japan Transport Safety Board, “2003-2012: Aircraft accident reports”, available at: <http://www.mlit.go.jp/jtsb/>, 2020.
- 467 Kikuchi, R., Misaka, T., and Obayashi, S.: Real-Time Flow Prediction of Low-Level Atmospheric Turbulence, 33rd
468 Wind Energy Symposium, 2015.
- 469 Kameyama, S., Ando, T., Asaka, K., Hirano, Y., and Wadaka, S.: Compact all-fiber pulsed coherent Doppler lidar
470 system for wind sensing, Applied Optics, 46.11, 1953-1962, 2007
- 471 Machida, S.: Project Overview of R&D for Onboard Turbulence Detection System, Proceedings of Asia-Pacific
472 International Symposium on Aerospace Technology 2017, Plenary Lecture 4 (Seoul, Korea, 2017).
- 473 Misaka, T., Nakabayashi, F. K., Obayashi, S., and Inokuchi, H.: Filtering Algorithm of Airborne Doppler Lidar
474 Measurements for Improved Wind Estimation, Transactions of the Japan Society for Aeronautical and Space
475 Sciences, 58.3, 149-155, 2015
- 476 Newsom, R. K., et al.: Validating precision estimates in horizontal wind measurements from a Doppler lidar,
477 Atmospheric Measurement Techniques (Online) 10. NREL/JA-5000-68401 (2017).
- 478 Regan, C.D., and Jutte, C.V. (2012), Survey of applications of active control technology for gust alleviation and new
479 challenges for lighter-weight aircraft. NASA Technical Memorandum, NASA-TM-2012-216008.
- 480 Saito, K., Ishida, J. I., Aranami, K., Hara, T., Segawa, T., Narita, M., and Honda, Y, Nonhydrostatic atmospheric
481 models and operational development at JMA, Journal of the Meteorological Society of Japan 85B, 271-304, 2007.



482 Schmitt, N. P., Rehm, W., Pistner, T., Zeller, P., Diehl, H., and Navé, P.: The AWIATOR airborne LIDAR
483 turbulence sensor, *Aerospace Science and Technology*, 11.7, 546-552, 2007
484 Sermi, F., Cuccoli, F., Mugnai, C., and Facheris, L.: Aircraft hazard evaluation for critical weather avoidance,
485 *Metrology for Aerospace (MetroAeroSpace)*, IEEE, 2015.
486 Soreide, D. C., Bogue, R. K., Ehernberger, L. J., Hannon, S. M., and Bowdle, D. A.: Airborne coherent LIDAR for
487 advanced in-flight measurements (ACLAIM) flight testing of the LIDAR sensor, NASA Technical Reports, 2000.
488 Woltring, H. J.” A Fortran package for generalized, cross-validatory spline smoothing and
489 differentiation.“ *Advances in Engineering Software*, 8.2, 104-113, 1986
490